ELSEVIER

Contents lists available at ScienceDirect

Chemical Engineering Science

journal homepage: www.elsevier.com/locate/ces





Linear solvation energy relationships for adsorption of aromatic organic compounds by microplastics

Dilara Hatinoglu^a, Abdulrahman Adan^b, Francois Perreault^{c,d}, Ipek Imamoglu^b, Onur G. Apul^{a,*}

- ^a Department of Civil and Environmental Engineering, University of Maine, Orono, ME 04469, USA
- ^b Department of Environmental Engineering, Middle East Technical University, Ankara, Turkey
- ^c School of Sustainable Engineering and the Built Environment, Arizona State University, Tempe, AZ 85281, USA
- d Department of Chemistry, University of Quebec in Montreal, CP 8888, Succ. Centre-Ville, Montreal, QC, H3C 3P8, Canada

ARTICLE INFO

Keywords: Adsorption LFER LSER Modelling Microplastics

ABSTRACT

This study develops predictive models for adsorption of organic compounds (OC) by microplastics using linear solvation energy relationship (LSER). The adsorption mechanism of aromatic OCs by microplastics was investigated by delineating the effect of molecular weight of the OCs, polymer type of MPs, and background water chemistry. The benchmark model for adsorption of OCs (n = 28) by polyethylene yielded an $R^2 = 0.85$ (n = 28), RMSE = 0.38, $Q^2LOO = 0.73$. Further narrowing the dataset down by decreasing the molecular weight cutoff to OCs < 192 g/mol improved the model to $R^2 = 0.98$ (n = 13). Validation techniques tested the predictive strength of the benchmark model, which included new experimental adsorption data and performing leave-one-out cross validation. Among LSER model descriptors, the molecular volume was the most predominant descriptor in all scenarios, suggesting the importance of non-specific interactions and OC hydrophobicity. The results demonstrated that LSER is a promising approach for predicting the adsorption of aromatic OCs by MPs.

1. Introduction

Plastics are practical, durable, low cost, and lightweight materials providing benefits to almost every industry imaginable (Crawford and Quinn, 2016; Sun et al., 2022; Shen et al., 2021). They are also imperative for food packaging, safe medical services, inexpensive clothing, clean water storage that improve the standards of life around the world. Therefore, since the 1950s, society's ever-increasing demand for plastics has boosted their global production rate by more than two orders of magnitude (Europe, 2021). During their environmental retention, plastic debris are exposed to natural weathering processes (e.g., UV irradiation, heat, mechanical stress, and biodisintegration), which break them down into microplastics (MPs) (Botterell et al., 2019). Given their small sizes within the optimal prey range (Galloway et al., 2017), MPs are mistaken by many aquatic species, resulting in intestinal damage (Lei et al., 2018), developmental inhibition (Zhang et al., 2022), energy budget disturbance (Wright et al., 2013); structural alterations, and oxidative stress (Vasanthi et al., 2021). Moreover, MPs are complex cocktails of polymers and chemical additives, which can be further exacerbated by the sorption of synthetic organic compounds (OCs) and pathogens owing to their high surface area and hydrophobicity (Galloway et al., 2017; Rochman et al., 2019; Huang et al., 2023; Liu et al., 2023). Thus, MPs are potential "Trojan Horses" for toxic pollutants; that could cause severe health implications (Pedà et al., 2016; Rainieri et al., 2018; Dong et al., 2023; Ricardo et al., 2021). In contrast, there has been conflicting evidence of decreased toxicity by the presence of MPs, proving that the ingestion of MPs is a negligible chemical uptake route compared to water exposure for fish (Schell et al., 2022). Therefore, it is imperative to explore the sorptive interactions between MPs and toxic OCs. These complex interactions are influenced by MP properties (e.g., size, shape, crystallinity, hydrophobicity, functional groups, and additives) (Mei et al., 2020; Wang et al., 2021), OC's characteristics (e.g., hydrophobicity, ionic property, and functional groups) (Li et al., 2018; Zhang et al., 2018), and solution chemistry (e.g., ionic strength, pH, and natural organic matter) (Li et al., 2018; Ma et al., 2019; Scott et al., 2021; Wang et al., 2015). Given that all these factors concurrently affect the phase-transfer processes (ab- and adsorption), conducting laboratory experiments for 70,000 + OC is not practical. Currently,

E-mail address: onur.apul@maine.edu (O.G. Apul).

 $^{^{\}ast}$ Corresponding author.

equilibrium constants (K_d) for MPs are determined by sorption experiments, which take long equilibrium time, require trained staff, and lead to excessive cost. Developing predictive models based on solvation theory not only provides K_d values, but also unravels the sorption mechanism. Moreover, unraveling the mechanisms of the sorption process between MPs and OCs can provide insights for developing effective treatment technologies because plastics are commonly used in water and wastewater treatment plants as resins (e.g., polystyrene, acrylic polymers).

The partitioning of OCs to MPs can take place by sorption, and the predominant mechanism varies for each polymer (Prajapati et al., 2022). OCs can diffuse into loosely arranged polymer chains of amorphous rubbery polymers (e.g., PE, PP) via absorption by weak van der Waals forces (Prajapati et al., 2022; Atugoda et al., 2020; Endo et al., 2016). On the contrary, they are restricted in glassy amorphous polymers (e.g., PS, PVC) due to highly dense, cross-linked molecular structures, which cease absorption into polymer matrix (Atugoda et al., 2020). Instead, glassy polymers have internal nanoscale pores creating strong adsorption sites for OCs (Hartmann et al., 2017). Adsorption is generally the predominant process at low concentrations of OCs, while absorption takes over at high concentrations due to larger volume requirement to accommodate molecules (Prajapati et al., 2022; Hartmann et al., 2017). Bearing in mind that polymer structure and OCs' concentration in water are closely linked to the predominant mass transfer mechanism (adsorption and/or absorption), we refrained from differentiating the terms and used the term 'sorption' because this study aims at identifying the partitioning of OCs in a biphasic watermicroplastic system (Endo et al., 2016; Hartmann et al., 2017).

Equilibrium constants can be predicted using single-parameter free energy relationships either based on octanol-water (log Kow) or hexadecane-water distribution coefficients (log K_{hw}). However, wide diversity of chemicals makes single parameter approach insufficient and more comprehensive multiple parameter tools considering multiple aspects of solutes are needed to make more precise predictions (Hüffer et al., 2018). Abraham's linear solvation energy relationship (LSER) approach allows the investigation of individual molecular interactions and their contribution to overall sorption. Since 1990s, this approach has been used to predict adsorption of a variety of compounds by multiwalled carbon nanotubes (CNTs) (Apul et al., 2013; Ersan et al., 2016; Hüffer et al., 2014), single-walled CNTs (Apul, 2014; Wu et al., 2016), graphene (Xia et al., 2010), graphene oxide (Ersan et al., 2019), and black carbon (Su et al., 2018). Up to now, only four studies have used LSER approach to model the sorption of organic compounds by MPs (Hüffer et al., 2018; Wei et al., 2019; Xu et al., 2021; Hatinoglu et al., 2023). Poly parameter approach has shed light on exploring the sorption mechanism in terms of the characteristics of the polymer, OCs, and water type. The first study developed a model for the adsorption of 21 different OCs containing aliphatic and aromatics onto UV-aged PS MPs, yielding $R^2 = 0.95$ (Hüffer et al., 2018). In line with most LSER studies using polymeric sorbents, hydrophobic attraction of OCs towards MPs was the most reported as the significant adsorption mechanism. Furthermore, OCs' tendency to make H-bonds with water was higher than with UV-aged PS MPs because of oxygen-containing surface groups on aged PS MPs, which decreases the availability of sorption sites to MPs (Hüffer et al., 2018). The second study broadened the understanding by developing LSER models for different polymer types in different matrices, covering sorption by PE in seawater (n = 36, R^2 = 0.91), PE in freshwater (n = 36, R^2 = 0.91), PE in pure water (n = 35, R^2 = 0.98), and PP in seawater (n = 35, R^2 = 0.96). For all three PE models, hydrogen bond basicity and cavity formation effect were the governing mechanisms. For the PE in the seawater model, induced dipole effect was another prevailing mechanism due to high salinity. Unlike other polymers, sorption by PP in seawater was not significantly affected by cavity formation energy, which was attributed to the high crystallinity of PP (due to the methyl groups), reducing the energy need for cavity formation. In the third study, it was found for the first time that

intermolecular interactions governing the adsorption mechanisms may vary depending on the polarity of MPs (Xu et al., 2021). Even though the sorption by polar MPs involved less hydrophobic interactions and van der Waals forces than non-polars (i.e., PCL < PBS < LDPE < PS), they had much greater adsorption capacities due to making stronger polar interactions such as H-bonding and p/ π - π electron donor–acceptor interactions. In the most recent study, we introduced the applicability of LSER modelling for adsorption of ionizable perfluoroalkyl carboxylic acids (PFCAs) onto PS MPs by correcting Abraham's descriptors (Hatinoglu et al., 2023). Results showed that polarizability and hydrophobicity of anionic PFCA drive them to MPs while the van der Waals interactions between PFCA and water diminish PFCA's binding affinity. The study was the first attempt to develop models by compiling data from literature and comparing LSER results side by side for different polymer types and water types (Hatinoglu et al., 2023).

Furthermore, while previous efforts also elucidated the interactions between a wide range of organic compounds and water samplers and pipes (Uber et al., 2019; Uber et al., 2019; Egert and Langowski, 2022; Egert and Langowski, 2022), our study excluded the data pertaining bulk polymeric materials from our analysis to maintain the clarity and focus of our investigation on the MPs. As detailed in Table S1, no study has accomplished providing such mechanistic insights yet. This study introduces new perceptions to predictive model development literature by performing systematic data gathering, and classification aiming at data homogeneity. This novel approach enables conveying predictions specific to each element of sorptive interactions between MPs and OCs, by changing only one variable at a time.

The objectives of this study are to investigate the mechanisms and the corresponding impacts of: (i) OCs' molecular weight; (ii) MPs' polymer type; and (iii) background water type on the adsorption of OCs by MPs using LSER approach and by comparing our findings within the literature. Moreover, LSER models were internally validated, and experimental adsorption data was generated to externally validate the benchmark model.

2. Materials & methods

2.1. OCs and MPs used for model training

An exhaustive literature review was conducted to compile all the partition coefficients ($\log K_D$) related to the sorption of neutral aromatic OCs by PE MPs in deionized water. Log K_D values at the Henry's region (i.e., most linear portion) of the isotherms were analyzed to represent sorption at diluted concentrations. Moreover, the last data points in isotherms were used to calculate $\log K_D$ values at saturated concentrations. The linear partition model allowing the attainment of K_D values is given in eq. (1):

$$q_e = K_D \bullet C_e \tag{1}$$

Where q_e is the amount of adsorbate on the MPs (mg/g), C_e is the amount of adsorbate remaining in the solution (mg/L), and K_D is the linear partition coefficient (L/kg) under equilibrium. Partition coefficients obtained from the two ends of the isotherm were used to test the impact of surface area normalization on model predictivity.

Four classification criteria were implemented for OC and MP type selection. First, modelling efforts were focused on aromatic compounds because most data are for aromatics in literature. Second, ionized compounds were out of the scope of this study as traditional LSER models are not capable of predicting them. Third, only the data associated with virgin MPs were considered and the ones undergone any natural (i.e., MPs extracted from an environmental media) or artificial (e.g., UV irradiation, ozonation) weathering process were omitted from the study as surface functionalization of MPs can affect the adsorption interactions of OCs (Hüffer et al., 2018; You et al., 2021). Fourth, datasets were not narrowed down to particle sizes because MP sizes were found not to be a limiting factor for the adsorption process.

Following these assumptions yielded a database containing $\log K_D$'s for the sorption of 31 neutral aromatic OCs from 18 studies and it was used to examine the impact of OCs' molecular weight (MW) on the sorption process (Table S2). Figure S1 shows the MW distribution of 31 OCs in the database. The right-skewed histogram indicates that most OCs in the dataset has MWs in lower range. MW is related to OCs' molecular volume, and it is the most influential parameter in adsorption process (Apul et al., 2013; Apul et al., 2020). Therefore, the database was first subgrouped into seven different MW cutoffs by excluding three of the largest MW OCs from the dataset systematically for each cutoff. Then, the prediction strengths of seven models were compared and the model yielding highest R^2 with greatest number of data points was selected as the benchmark model (MW < 404 g/mol, $R^2 = 0.85$, n = 28). Furthermore, the benchmark model was verified by internal and external validation techniques as described in Section 2.3.

The second database was generated to examine the impact of polymer type and contained data for adsorption of 25 aromatic OCs by PS MPs, which are all contained in the starting database as well. Among 25 compounds, 22 of them were at the same MW cutoff with benchmark model (<404 g/mol) (Table S3). Therefore, the models created for the sorption of same 22 compounds by PE and PS were compared side by side (log K_D values are given in Table 2).

Finally, two more datasets were generated for the sorption of 17 PCB by PE MPs in freshwater and seawater to examine the impact of water type (Table 3). Here, the freshwater was a synthetically prepared solution containing calcium chloride, magnesium sulfate, sodium hydrogen carbonate, and potassium hydrogen carbonate, while seawater was a real sample with salinity of 3.4% and dissolved organic carbon (DOC) of 0.17 mg/L. Moreover, the diameter of PE microspheres was $99\pm39~\mu m$ (Velzeboer et al., 2014).

2.2. Descriptor collection

Abraham's LSER approach is used to create a linear poly parametric model and describe solvation or directly related activities by using compounds' physicochemical properties. The model provides mechanistic insights because it reveals the intermolecular interactions between the sorbent and sorbates as well as quantifying their relative individual contribution to the sorption process. A typical LSER model that describes the sorption of neutral OCs is given in eq (2):

$$Log K_D = c + eE + sS + aA + bB + vV$$
 (2)

where 'log K_D ' is partitioning coefficient between MPs and water under equilibrium conditions; 'E' is the excess molar refraction in units of (cm³ mol $^{-1}$)/10 representing non-specific van der Waals forces; 'S' is the polarizability/dipolarity parameter, 'A' and 'B' are the hydrogen bond donating (acidity) and accepting (basicity) abilities, respectively; and 'V' is the molecular volume or McGowan's volume in units of (cm³ mol $^{-1}$)/100. Lastly, 'c' is the regression constant, and 'e', 's', 'a', 'b', and 'v' are the fitting coefficients indicating the contribution of each interaction on the adsorption mechanism (Xu et al., 2021; Apul et al., 2020). In this study, all solvatochromic descriptors were obtained from the Helmholtz Centre for Environmental Research (UFZ) database (Ulrich et al., 2022). Figure S2 shows the descriptors that were used as independent variables to train our benchmark model.

2.3. Statistical methods for model development and evaluation

Paired t-test was performed to compare $\log K_D$ values of different datasets. Multiple linear regressions were conducted by assigning $\log K_D$ as dependent variable and Abraham solvation descriptors as independent variables using Microsoft Excel. The regression models were evaluated by the p-values obtained from analysis of variance (ANOVA). Independent variables with a p-value less than 0.05 were accepted as statistically significant in predicting the dependent variable. The multicollinearity of independent variables was quantified by variance

inflation factor (VIF) as shown in eq (3):

$$VIF = \frac{1}{1 - r_i^2} \tag{3}$$

where, r_i^2 is the squared correlation coefficient of the ith coefficient when the ith descriptor was regressed against all other descriptors. Higher VIF values indicated more severe correlations with one or more of the remaining independent variables. The independent variables were accepted as correlated if the VIF values were larger than 10 (Midi et al., 2010). The goodness of the fit was examined by the coefficient of determination (R^2). The predictive precision of the models was quantified by the root mean squared error (RMSE) as shown in eq (4):

$$RMSE = \sqrt{\frac{\sum_{i=1}^{n} (y_i - \hat{y}_i)^2}{n}}$$
 (4)

where, n is the number of compounds in the training set. y_i and \hat{y}_i are experimental and predicted log K_D values for the ith compound in the training set, respectively. RMSE is used to measure the distance between predicted and actual values, and so it quantifies how concentrated the data is around the line of best fit. Smaller RMSE values indicated a stronger prediction tendency of a model.

2.3.1. Internal validation

Two different internal validation techniques were used to evaluate the robustness of the benchmark model. First, the benchmark dataset (n = 28) was ranked in decreasing order of $\log K_D$ values; 21 compounds were then selected for the training and 7 for validation of the LSER model by following the randomization pattern of VTTT (V: validation; T: training).

Second, leave-one-out (LOO) cross validation was carried out by using the benchmark model's dataset. In this technique, each compound was left out once and an LSER model was fit with the remainder of the data until all 28 compounds had been predicted. RMSE of LOO (RMSE $_{LOO}$) and LOO validated R² (Q $_{LOO}^2$) were calculated as the criterion. Q $_{LOO}^2$ was calculated using eq (5):

$$Q_{LOO}^{2} = 1 - \frac{\sum_{i=1}^{n} (y_{i} - \widehat{y}_{i})^{2}}{\sum_{i=1}^{n} (y_{i} - \overline{y}_{i})^{2}}$$
 (5)

where, \overline{y} is the average experimental log K_D value of the training set. A high value of Q_{LOO}^2 ($Q_{LOO}^2 > 0.5$) was considered as proof of the high predictive ability of the model (Ding et al., 2016).

In addition to the benchmark model, LOO cross validation was also carried out for the models shown in Fig. 4 and Fig. 5. Cross validation results are shown in Figure S5.

2.3.2. External validation

For external validation, isotherms were experimentally generated for the sorption of triclosan and 2,3,6-trichlorophenol by PE MPs. The predictive precision of the benchmark model was evaluated by calculating RMSE. PE MPs (density: 0.935 g/cm³) used in sorption experiments were purchased from a local water tank manufacturer in Turkey in shredded form, and characterization was performed by METU Central Laboratory. The polymer type was confirmed by diamond crystal ATR-FTIR analysis using IFS/66S, Hyperion 1000. The crystallinity and melting temperature (T_m) of PE were measured by Perkin Elmer Diamond Differential Scanning Calorimetry (DSC) (Heating rate: 10 °C/ min, Temperature range: 30 °C to 300 °C, Under N2 atmosphere). Specific surface area of MPs was measured using multi-point N2 BET method (for 24 h degassing at 50 °C). Particle size distribution of MPs was determined by using ASTM method (Astm, 2017), which involved passing the MPs through a stack of sieves with mesh openings ranging from 2.0 to 0.106 mm, and weighing the particles retained on each sieve (Astm, 2017). Finally, zeta potential of PE was measured to determine the point of zero charge (pHpzc) using MALVERN Nano ZS90. The characteristics of MPs are summarized in Table 1 and the detailed results

Table 1Characteristics of PE MPs used in validation experiments.

Density	T _m Crystallinity		SSA	pH_{pzc}	Particle size	
0.935 g/cm ³	126 °C	49.4%	$0.103 \text{ m}^2/\text{g}$	~2.2	250–500 μm	

T_m; melting temperature; SSA: specific surface area; pH_{pzc}: point of zero charge.

are given in Figure S6.

Triclosan (MW: 289.5 g/mol) and 2,3,6-trichlorophenol (MW: 197.4 g/mol) were two aromatic OCs selected to conduct sorption experiments for external validation of the benchmark model. These compounds fit the benchmark model because (i) their MWs are <404 g/mol and (ii) they are neutral at experimental conditions (pH = 6 for triclosan and pH = 4 for 2,3,6-trichlorophenol). The benchmark model was already trained by literature sorption data for triclosan, while no 2,3,6-trichlorophenol data was contained in the model training. Physicochemical properties of both compounds are given in Table S4.

Isotherm experiments for triclosan and PE MPs were performed by changing the MP amount (i.e., solid: liquid, S/L) in the sorption vials (i. e., 0.5, 1, 2, 4, 5, 10, 15, 20 g/L). Prepared amber vials were shaken horizontally at 200 rpm and 25 °C \pm 2 °C via incubating shaker (N-Biyotek NB-205 VL model). It was observed from kinetic sorption experiments that the equilibrium time was 24 h for triclosan at pH 6 (Figure S7). As experimental pH was smaller than its pKa, triclosan existed in its undissociated form. The same shaking conditions were also applied for 2,3,6-trichlorophenol, but initial pH was 4. Sorption isotherm experiments for 2,3,6-trichlorophenol and PE MPs were performed by changing the initial concentration from 1 to 60 ppm at pH = 4, where the compound existed in its undissociated form. Tricosan and 2,3,6- trichlorophenol were measured directly using a UV/Vis Spectrophotometer (HACH DR6000) at the wavelength of their maximum absorbance, i.e., 279 and 289 nm, respectively.

Table 2 Comparison of polymer type for $\log K_D$ values using the compounds in benchmark model (n = 28) and model for sorption by PS MPs (n = 22) in deionized water at MW cutoff 404 g/mol.

C1	MW	les V	$\log K_D$		
Compound	(g/mol)	log K _{ow} -	PE	PS	
carbendazim	191.2	1.50	0.7	n/a	
carbofuran	221.3	1.97	2.4	n/a	
diethyl phthalate	222.2	2.47	1.4	1.1	
atrazine	215.7	2.61	2.2	n/a	
diuron	233.1	2.68	1.8	0.3	
triadimefon	293.8	2.77	2.1	n/a	
1-naphthol	144.2	2.85	1.2	1	
bromobenzene	157.0	2.99	2.2	2.7	
azoxystrobin	403.4	3.09	2.3	2.4	
benzophenone-3	244.2	3.18	2.8	2.8	
1-nitronaphthalene	173.2	3.19	2.2	2.2	
m-xylene	106.2	3.20	2.1	3.3	
naphthalene	128.2	3.30	2.7	3	
bisphenol A	228.3	3.32	0.5	-0.1	
2-tertbutyl-4-methyl phenol	164.2	3.60	1.8	1.6	
n-propylbenzene	120.2	3.69	2.7	3.7	
picoxystrobin	367.3	3.83	2.6	2.4	
1-methylnaphthalene	142.2	3.87	3.1	3	
2,3,5-trimethyl phenol	136.2	4.00	1.5	1.4	
1-chloronaphthalene	162.6	4.00	3.4	3.2	
biphenyl	154.2	4.01	3.2	3.3	
17B-estradiol	272.4	4.01	2.4	2	
diisobutyl phthalate	278.3	4.11	3.2	4	
pyraclostrobin	387.0	4.23	3.7	3.8	
phenanthrene	178.2	4.46	4.2	3.6	
dibutyl phthalate	278.3	4.50	3.4	3.8	
triclosan	289.5	5.00	2.8	n/a	
dichlorodiphenyltrichloroethane	354.5	6.36	5.1	n/a	

^{*}Compounds were ranked in ascending order of their log K_{ow} values. n/a: not available.

Colored bars were obtained by conditional formatting, and they demonstrate relative magnitude of $\log K_D$ values of PE and PS.

3. Results & discussion

3.1. Overview of literature for sorption of OCs by MPs

Table 2 compares $log K_D$ values of PE and PS MPs at MW cutoff < 404 g/mol. In general, the log K_D values for both polymers showed a relationship with $\log K_{ow}$ values of OCs indicating the important role that hydrophobic interactions play in sorption. Although the polymer structures of PE and PS differ greatly, there is no statistically significant difference between the $\log K_D$ values of 22 neutral aromatic OCs by PE and PS MPs (p > 0.05). This indicates that sorption by MPs may not be mainly controlled by polymer related properties. PE is a simple linear molecule and a rubbery amorphous polymer (i.e., glass transition temperature, Tg, is below ambient temperature, Tamb) that can absorb compounds uniformly due to the relatively high flexibility of polymer segments (Atugoda et al., 2020; Endo et al., 2016). In contrast, PS is a glassy amorphous polymer (T_g > T_{amb}) containing benzene groups in its structure. Sorption by PS MPs is rather an adsorption-like or pore-filling process resulting in nonlinear isotherms to occur (Endo et al., 2016). Contrary to literature (Wei et al., 2019), benzene group of PS making π - π interactions with aromatic OCs did not cause PS to exhibit significantly higher $\log K_D$ values than PE. Additionally, PE MPs' ability to induce diffusion of OCs into polymer matrix did not help them surpass sorption capacity of PS MPs. A more conclusive side by side comparison would only be possible if the MPs' size, shape, additive content, and surface oxygen contents were kept constant.

Table 3 compares $\log K_D$ values of 17 PCBs for PE MPs in seawater and freshwater. In general, $\log K_D$ and $\log K_{ow}$ values of PCBs increase with MW of compounds in both water types. Moreover, the distribution pattern of $\log K_D$ values for each PCB is the same for each water type. For most PCBs, sorption by PE MPs was greater in seawater than in freshwater, and the difference between the entire groups was statistically significant at the 95% confidence level. The improved sorption affinity in seawater has also been previously reported for PFAS and was attributed to salting out effect (i.e., decreasing water solubility of PFAS) or cation bridging in the presence of ions in seawater (Llorca et al., 2018). Unlike PFAS, PCBs exist in neutral forms at experimental pH and their water solubility is very low, therefore mechanisms leading to this

Table 3 Comparison of water type for $\log K_D$ values using 17 PCB adsorbed by PE MPs in seawater and freshwater.

C 18	MW	log V	$\log K_D^{\ \mathrm{b}}$			
Compound ^a	(g/mol)	$\log K_{ow}$	Seawater	Freshwater		
PCB-28	257.5	5.7	6.2	5.3		
PCB-31	257.5	5.7	6.1	5		
PCB-44	292.0	5.8	6	5		
PCB-52	292.0	5.8	6	5.1		
PCB-74 ^c	292.0	6.2	6.8	5.9		
PCB-77 ^d	292.0	6.4	5.8	6.2		
PCB-101 ^c	326.4	6.4	6.6	5.6		
PCB-105	326.4	6.4	6.8	6.2		
PCB-118	326.4	6.7	6.3	6.3		
PCB-126 ^d	326.4	6.7	7	6.7		
PCB-149	360.9	6.7	6.2	6.2		
PCB-138 ^c	360.9	6.8	6.7	6.9		
PCB-153 ^c	360.9	6.9	7.6	7.1		
PCB-156	360.9	7.2	7.8	7.2		
PCB-170	395.3	7.3	8	7.3		
PCB-169 ^d	360.9	7.4	8.3	7.8		
PCB-180 ^c	395.3	7.4	7.9	7.4		

 a Compounds were ranked in ascending order of their log K_{ow} values; b Data from (Velzeboer et al., 2014); c non-planar PCB; d planar PCB; n /a: not available. Colored bars were obtained by conditional formatting, and they demonstrate relative magnitude of log K_{D} values of PE in seawater and freshwater.

behavior should be different, such as DOC content of seawater. Moreover, planar PCBs are sorbed by PE stronger than non-planar PCB congeners because they can move closer to the surfaces (Velzeboer et al., 2014).

Fig. 1 shows the log K_{ow} (octanol–water partition coefficient) versus log K_D values for compounds at MW cutoff < 404 g/mol. The correlations for PE (R² = 0.58) and PS (R² = 0.39) indicate that the sorption of OCs by MPs cannot be explained by hydrophobic interactions alone. It is necessary to consider the impact of multiple parameters (e.g., sorbent and solute related properties) simultaneously to predict the sorption mechanism. In contrast, the correlation for PCB was comparatively higher as they are a family of compounds. Especially, it was stronger for freshwater (R² = 0.94) than in seawater (R² = 0.72), indicating that the interactions in seawater can be more complex than in freshwater relying mainly on hydrophobic sorption. In seawater, dipole interactions may be observed between salt ions and MPs' surfaces, that may weaken the correlation. This speculation will be further tested later and elaborated more in Section 3.5.

3.2. Training and internal validation of benchmark model

The impact of OCs' MW on LSER models was investigated using the datasets with different MW cutoffs. The model parameters obtained from the sorption by PE MPs in deionized water are shown in Table 4. Excluding three compounds with highest MWs from 31 aromatic OCs (Figure S3) remarkably changed the model predictivity in terms of (i) $\rm R^2$, (ii) relative importance of coefficients, and (iii) the sign of coefficients. From MW cutoff < 544 to < 404 g/mol, $\rm R^2$ increased from 0.50 to 0.85 and it was the most significant improvement achieved by MW cutoff testing. $\rm R^2$ value stayed almost stable until MW cutoff < 223 g/mol, and it reached to its maximum value (i.e., 0.98) at MW cutoff < 192 g/mol. This can be attributed to the increasing similarity of OCs as it was shown in right-skewed histogram (Figure S1), but not to changes in the number of OCs because adjusted $\rm R^2$ values' trend is parallel with $\rm R^2$. Despite the

very high goodness of the fit, the number of data (n = 13) was small which would limit the application domain of the developed model. Therefore, MW cutoff < 404 g/mol was selected to be the benchmark model of this study. While 'E' and 'S' were insignificant terms in the model of the raw dataset (n = 31), all five descriptors turned out to be significantly influencing the sorption process in the benchmark model (p < 0.05). However, it should be noted that there are only three OCs and to determine an actual MW cutoff, more data points are required.

Fig. 2a demonstrates the relative distribution of regression coefficients in the benchmark model (<404 g/mol, n=28) and Fig. 2b depicts the corresponding plot of experimentally measured vs. predicted $\log K_D$ values generated by this dataset (RMSE = 0.38). In this model, 'v' was the most influential parameter and positively correlated with the sorption process, indicating the importance of hydrophobic or nonspecific interactions between OCs and PE MPs. It implies that adsorption capability onto MPs increases as the compounds get larger. The second and third most significant coefficients were 'b' and 'a', respectively and were both negatively correlated with the sorption. This can be attributed to the capability of PE MPs for making H bond interactions with OCs is lower than that of bulk water. This agrees with the polymer's nonpolar property (-CH₂), and the virgin structure not containing any functional groups that can make hydrogen bonds with OCs. The term 's' was the fourth strong factor and negatively correlated with the adsorption, meaning that dipolarity of OCs does not favor their sorption to MPs. It can be ascribed to that MPs have much lower dipolarity compared to water, causing them to have a weaker ability for making dipole/induced-dipole interactions with OCs. Finally, the slightly positive 'e' indicates that OCs has greater ability for polarizing effects toward PE MPs than bulk water. The model that Wei et al. (2019) developed for adsorption by PE MPs in deionized water has similarities with our benchmark model in terms of dominating descriptors and their signs, which are descriptor 'V' and 'B'. Contrary to ours, that study omits 'A', 'E' and 'S' in their model due to having a dissimilar training dataset that contains both aliphatic and aromatic OCs. On the other hand, the

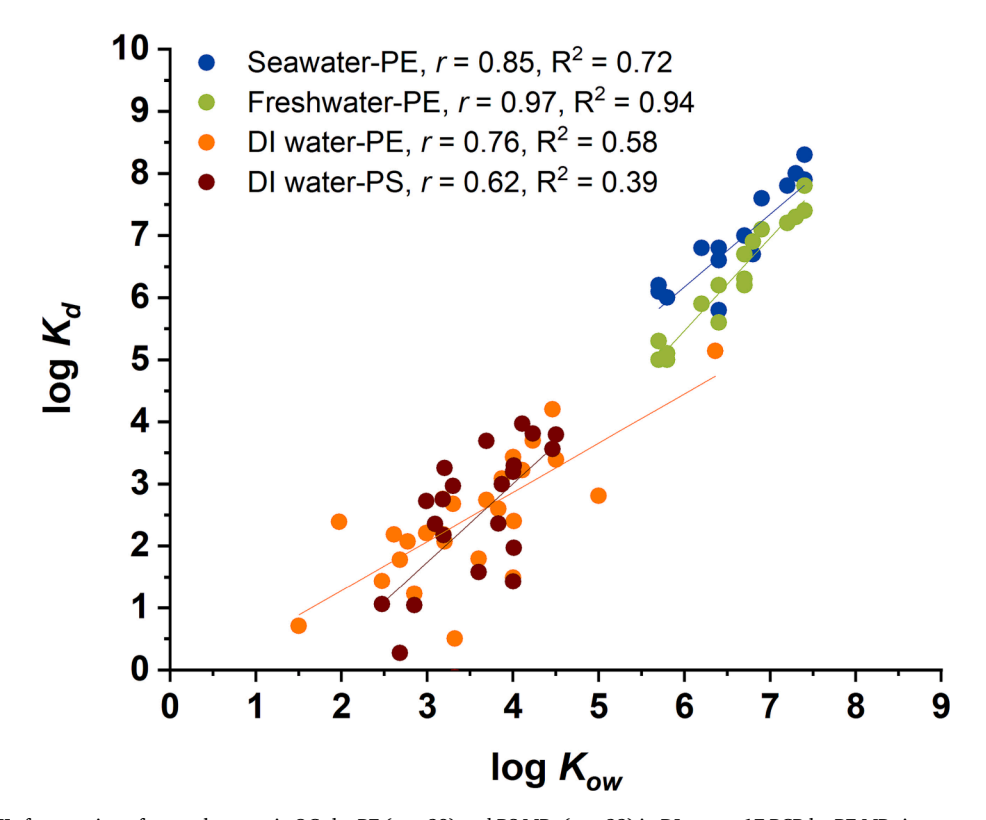


Fig. 1. Log K_{OW} vs. log K_D for sorption of neutral aromatic OCs by PE (n = 28) and PS MPs (n = 22) in DI water, 17 PCB by PE MPs in seawater and freshwater at MW cutoff < 404 g/mol. r: the Pearson correlation coefficient and R^2 : the coefficient of determination.

Table 4
LSER model parameters for the sorption of neutral aromatic OCs by PE MPs in deionized water at different molecular weight cutoffs

MW cutoff*	n	\mathbb{R}^2	R^2_{adj}	c	e	s	a	b	v	Significant terms (p<0.05)
< 544	31	0.50	0.39	1.3 ± 0.5	-0.2±0.4	0.5 ± 0.6	-1.6±0.5	-1.3±0.4	1.1 ± 0.5	c, a, b, v
<404	28	0.85	0.82	0.2 ± 0.4	0.8 ± 0.3	-1.2±0.5	-1.5±0.3	-2.2±0.3	2.6±0.4	e, s, a, b, v
<355	25	0.86	0.82	0 ± 0.4	1.1 ± 0.4	-1.6 ± 0.7	-1.7 ± 0.3	-1.9 ± 0.4	2.8 ± 0.4	e, s, a, b, v
<279	22	0.83	0.78	-0.1 ± 0.5	1.2 ± 0.4	-1.6 ± 0.7	-1.9 ± 0.3	-1.7 ± 0.5	2.8 ± 0.5	e, s, a, b, v
<245	19	0.84	0.77	0 ± 0.8	1.1 ± 0.4	-1.7 ± 0.7	-2.1±0.4	-1.7 ± 0.5	2.9 ± 0.8	e, s, a, b, v
<223	16	0.90	0.85	-0.8 ± 0.7	1.6 ± 0.4	-2.7 ± 0.7	-2.1±0.4	-1.7 ± 0.5	3.8 ± 0.7	e, s, a, b, v
<192	13	0.98	0.96	-0.7 ± 0.4	1.5 ± 0.3	-2.1 ± 0.4	-1.7 ± 0.3	-2.6 ± 0.4	3.5 ± 0.4	e, s, a, b, v

*Relative absolute significance of each coefficient is comparatively visualized in Figure S4. Shaded row shows the selected benchmark model.

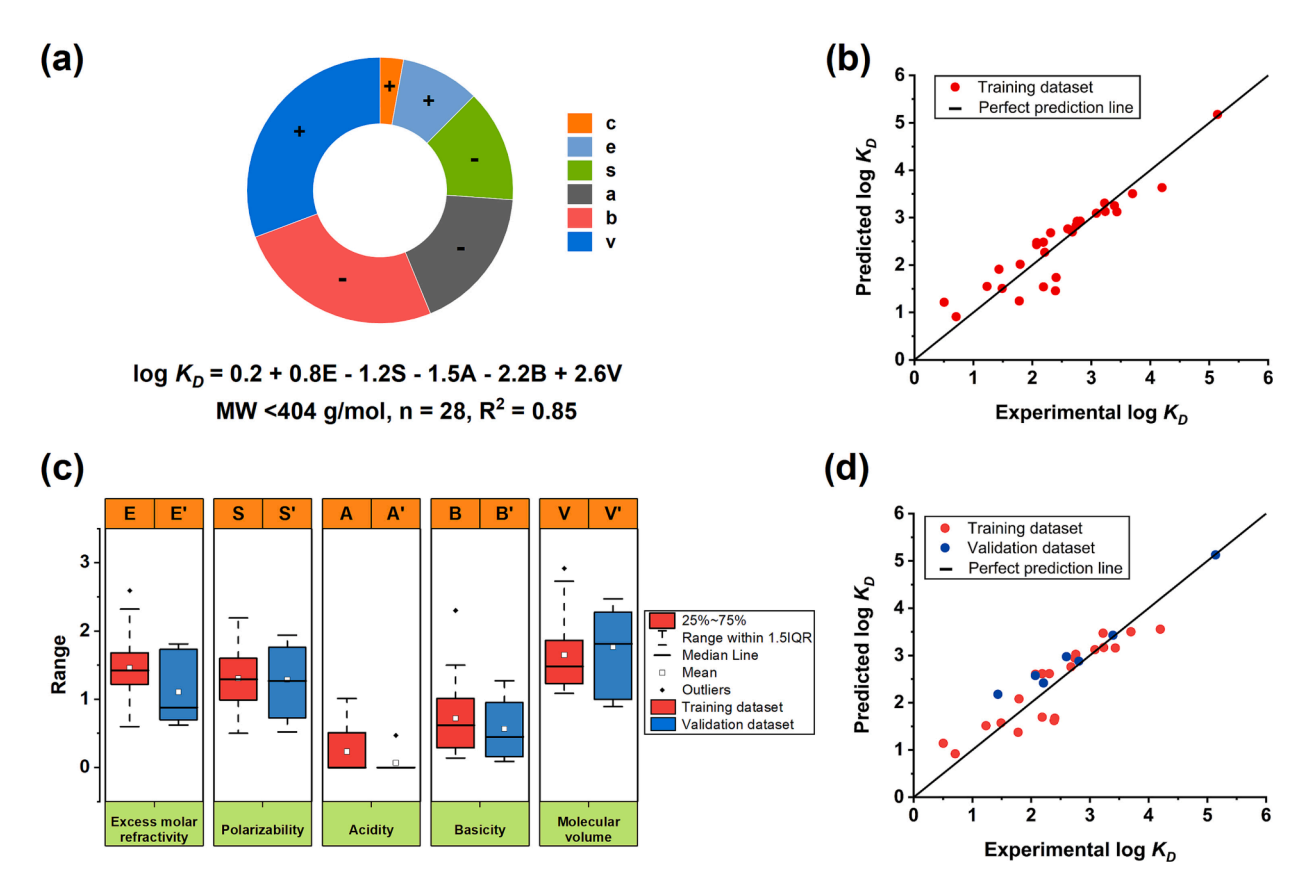


Fig. 2. (a) LSER equation and the corresponding regression coefficients' relative distributions in the benchmark model; (b) experimentally measured vs. predicted log K_D values generated by the combination of training and validation datasets (i.e., benchmark model, n = 28); (c) Box and Whisker plot for LSER descriptors of training (n = 21) and validation (n = 7, denoted by prime) dataset of benchmark model; (d) experimentally measured vs. predicted log K_D values for training and validation datasets.

model that Xu et al. (2021) developed for adsorption of 18 neutral aromatic OCs by LDPE MPs contains the same driving descriptors and signs with our study, but the coefficients' order of relative significance slightly differs at both equilibrium concentrations (i.e., 1 and 10% of water solubility). The similarities obtained from studies with different training datasets may be an indication of less complex interactions between OCs and PE MPs, especially when the medium is deionized water. Furthermore, although Egert and Langowski (2022)'s model was not specifically developed for MPs, the adsorption of a large group of compounds (n = 156, MW range = 32 to 722 g/mol) containing both aliphatic and aromatic OCs by LDPE films showed the same coefficient signs as our benchmark model but differed slightly in the significance order of the

descriptors. Table S5 compares the predictive strength of our benchmark model with Egert and Langowski (2022)'s model for our MW $<404~\mbox{g/mol}$ dataset.

Lastly, from 404 g/mol to lower MW cutoffs, the signs of descriptors do not change but relative importance of 'a', 'b' and 's' slightly changes (Table 4). This means that MW cutoff may not cause a fundamental change in the sorption process when compounds are smaller.

Then, the benchmark model was split into training (n = 21) and validation (n = 7) datasets for internal validation using VTTT approach. Fig. 2c shows the descriptors of randomized training and validation datasets and Fig. 2d shows the corresponding prediction curve. Here, log K_D values of 7 OCs were predicted using the model trained by 21 OCs.

Although the classification was randomized, the ranges of two sets' descriptors coincided with each other. This indicates that the training set includes a wide range of compounds and therefore can serve for the prediction of variety of compounds. This argument was supported by low RMSE value (RMSE = 0.38).

Finally, LOO cross validation (Figure S5) performed for the benchmark dataset (n = 28) resulted that RMSE $_{LOO}$ and Q_{LOO}^2 were 0.51 and 0.73, respectively. Low RMSE and high Q_{LOO}^2 ($Q^2 > 0.5$) proved the high predictive ability of the model (Ding et al., 2016).

3.3. External validation of the benchmark model

Fig. 3(a, b) shows two example adsorption isotherms produced for triclosan and 2,3,6-trichlorophenol, respectively. Sorption of both chemicals on MPs showed a good fit to Freundlich model with an R² of 0.986 and 0.976 for triclosan and 2,3,6-trichlorophenol, respectively.

As shown in Fig. 3(c), these two compounds lie in the interquartile ranges of training dataset's solvatochromic descriptors, therefore, it is likely that our external validation is within the applicability domain of the developed model. External validation of the benchmark model showed that log K_D of triclosan and 2,3,6-trichlorophenol can be predicted with 0.1 and 7.5% error, respectively (Fig. 3(d)). Moreover, RMSE for external validation set was 0.09. Despite the limited size of the external dataset, these statistical evaluations align with those of internal validation. This collective affirmation may demonstrate that the developed benchmark model is a potential tool for predicting the sorption of aromatic organic compounds with MW cutoff < 404 g/mol by PE MPs.

The reason for good external validation strength was traced back to the similarity in properties of PE MPs used in this study with those in literature. Figure S8(b) shows that MPs used in studies that make up our benchmark model has SSA ranging from 0.257 to 12.1 m²/g, particle sizes from 9.5 to 5000 μ m, and crystallinity from 35 to 61.5%. Our model MPs' particle size and crystallinity lie in the interquartile ranges, while SSA is even lower than the outlier of the literature data. Nevertheless, the developed LSER model was successful for predicting the experimental sorption data, which might be due to less importance of SSA in sorption of neutral aromatic OCs by PE MPs. The impact of SSA will be further investigated in Section 3.4 in surface area normalization of log K_D values.

3.4. The effect of MPs' surface area and polymer type on LSER models

Partition coefficients were normalized to examine whether surface area was a controlling factor for the sorption of aromatic OCs by PE MPs at MW cutoff < 404 g/mol using a common approach in literature (Apul et al., 2013; Apul et al., 2020; Zhou et al., 2015). This was only tested for 10 compounds as specific surface area information for MPs was only provided in those studies. Normalization efforts did not improve the model fitting indicating that surface area might not be a controlling factor, as also resulted in Section 3.3 (Table S6and S7). This has been observed in literature for different adsorbents such as single-walled CNTs (Apul et al., 2015), multi-walled CNTs (Apul et al., 2013), and graphene oxide (Shan et al., 2017) and was attributed to the much larger surface areas of the adsorbents compared to the necessary area required

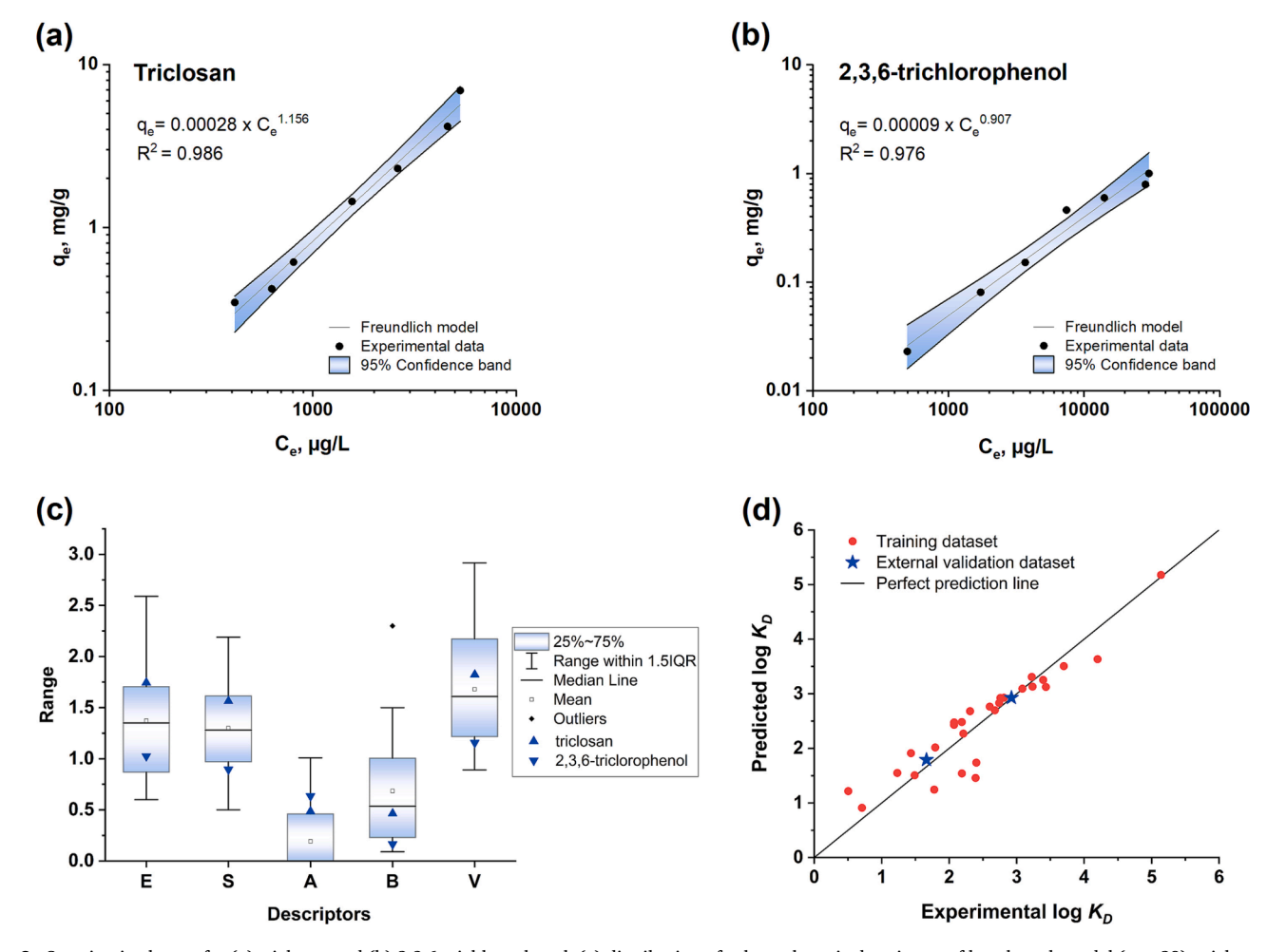


Fig. 3. Sorption isotherms for (a) triclosan and (b) 2,3,6-trichlorophenol; (c) distribution of solvatochromic descriptors of benchmark model (n = 28), triclosan and 2,3,6-trichlorophenol; (d) experimentally measured vs. predicted log K_D values for training and external validation datasets.

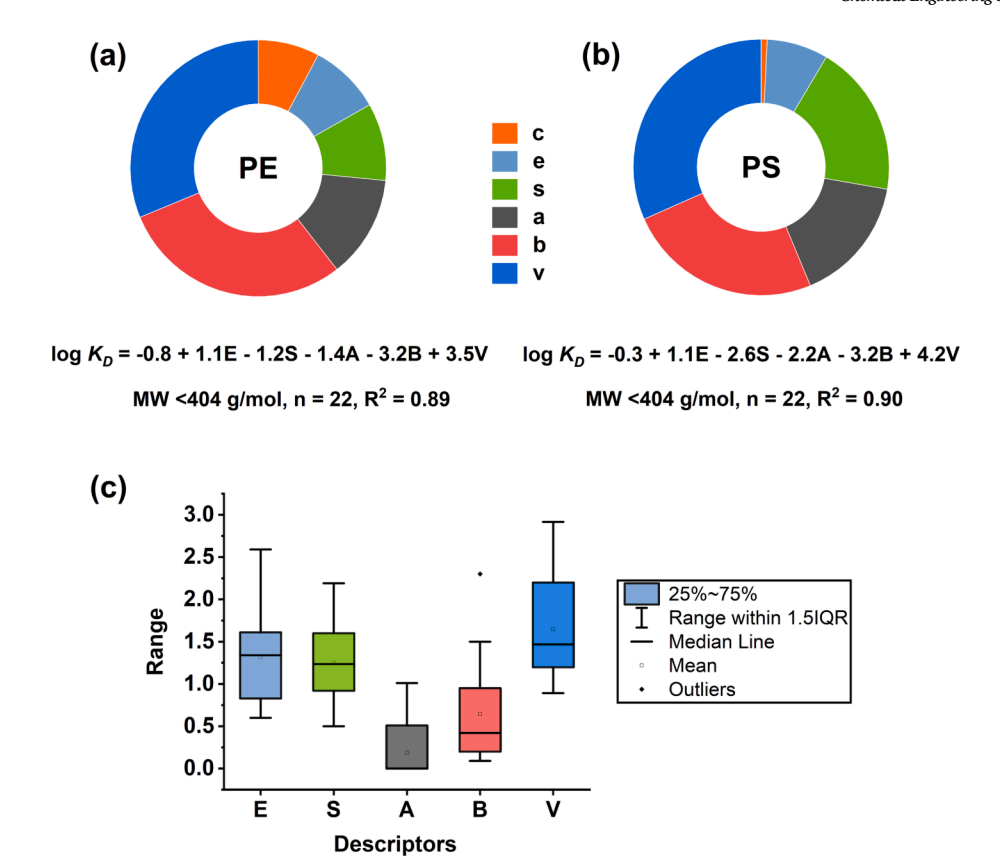


Fig. 4. LSER equations and the corresponding regression coefficients' relative distributions for (a) PE model (n = 22) and (b) PS model (n = 22); (c) Solvatochromic descriptors of 22 neutral aromatic OCs used in the models examining the impact of polymer type. All VIF values are smaller than 10, and the details are given in Table S8.

for accommodating each adsorbate on their surfaces. This evidence also supports our argument not to classify $\log K_D$ data based on particle sizes. However, it should be noted that the majority of first data points were<1% of OC solubility and the most saturated data point was<5% of OC solubility. At these concentrations, surface area may not be limited; thus, may not be controlling adsorption. At the plateau of the isotherm, the conclusion may change.

The impact of polymer type was examined by comparing two models for the sorption of 22 neutral aromatic compounds at MW cutoff < 404 g/mol by PE and PS MPs, which yielded similar prediction strength ($R^2 \cong 0.90$). Both models were internally validated using LOO approach, which resulted in $RMSE_{LOO} = 0.42$ and $Q^2_{LOO} = 0.77$ for PE and RMSE $_{LOO} = 0.51$ and $Q^2_{LOO} = 0.80$ for PS. Obtaining high values of $Q^2_{LOO} (Q^2_{LOO} > 0.5)$ for both models affirmed their high predictive strength. This enables us to make side by side comparison of the two models' outputs.

Fig. 4 shows the solvatochromic descriptors of compounds used to train these models and the corresponding regression coefficients. All 5 descriptors had statistically significant importance in both models because compounds' descriptors lie within a wide range (Fig. 4a). Furthermore, the relative contribution of each mechanism to sorption was determined by dividing the absolute values of each coefficient by the sum of all coefficients. Unlike PE, the parameter 's' was much more impactful than 'a' and 'e' in the PS model, and this has also been observed by Xu et al. (2021), where the models were developed for LDPE and PS MPs. This can be attributed to that although both MP types have weaker abilities of dipole/induced-dipole interactions with OCs compared to water, PS has less potential than PE. However, despite the differences in the two MPs' polymeric structure, the signs of coefficients did not change with the polymer type, which may conclude that the polymer chemistry does not primarily govern the compounds' affinity towards them, as the literature earlier reported for the comparison

between PS and LDPE MPs (Xu et al., 2021). This suggests that the benzene group of PS, along with its potential π - π interactions with aromatic OCs, does not appear to be strong enough to alter the direction of any of the adsorption mechanisms exhibited by PE MPs with the same set of OCs. However, more conclusive discussion can only be possible upon attainment of further MPs-related information.

3.5. The effect of water type on LSER models

The impact of water type was examined by comparing two models for the sorption of 17 PCB by PE MPs in freshwater (synthetic) and seawater at MW cutoff < 404 g/mol. The goodness of fit for the freshwater model ($R^2 = 0.89$, RMSE = 0.29) surpassed that of seawater ($R^2 =$ 0.65, RMSE = 0.47), which can be attributed to the DOC content and salinity of seawater, complicating the interactions due to dissimilar responses of PCB congeners. Fig. 5 shows the solvatochromic descriptors of compounds used to train these models and the corresponding regression coefficients. Descriptors 'A' and 'B' of PCBs had such a narrow range that they did not have a meaningful contribution to the model predictivity and thus were excluded from the model equations. In the freshwater model, 's' was the most influential parameter which was followed by 'v' and 'e'. In seawater, the relative absolute significance of 'v' was slightly higher than 's', and 'e' was the least important parameter. The coefficients' signs were the same in both models, indicating that water type is not reversing the direction of the interactions between compounds and MPs. The relative importance of 'e' and 's' were the same for both models, meaning that the strength of PE MPs' polarizing effect towards PCBs is not influenced by water type. Moreover, both freshwater and seawater are highly dipolar while PE has a much weaker ability for dipole/induced-dipole interactions. Therefore, the difference in water chemistry of the two water types might not trigger dipolar

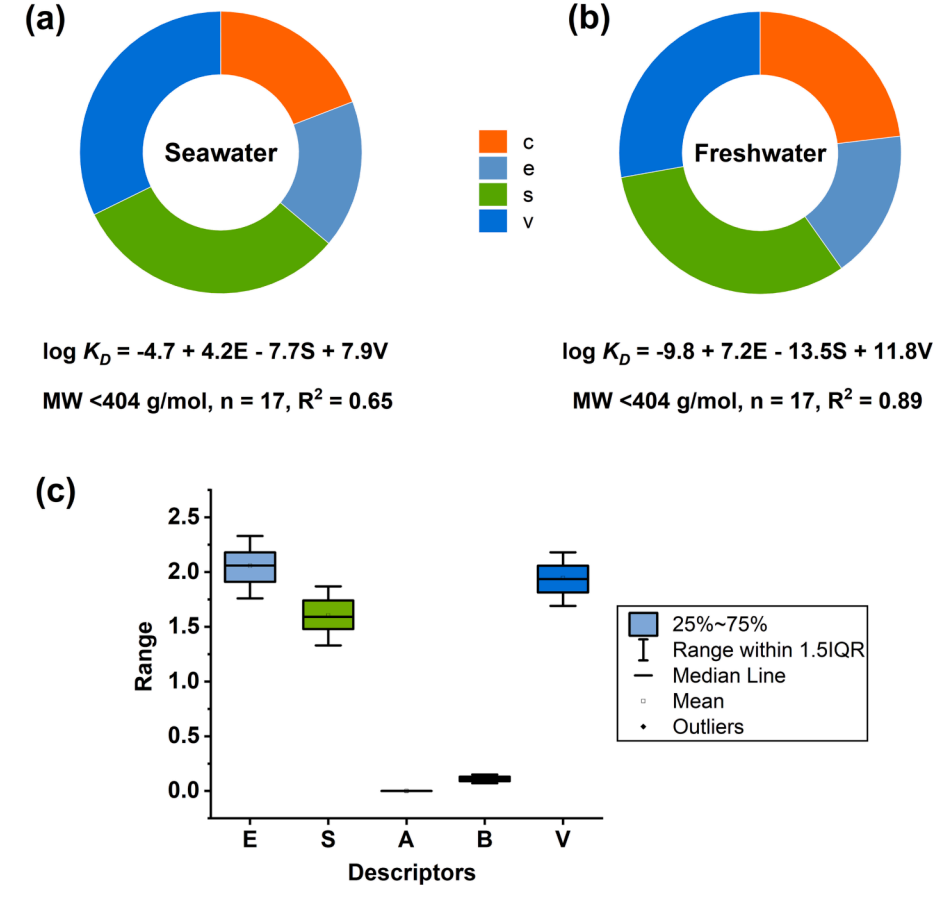


Fig. 5. LSER equations and the corresponding regression coefficients' relative distributions for (a) seawater model and (b) freshwater model. (c) Solvatochromic descriptors of 17 PCB used in the models examining the impact of water type. All VIF values are smaller than 10, and the details are given in Table S7.

interactions. 'v' was the only parameter rendering the sorption of PCB by PE MPs being higher in seawater than that in freshwater, which was supported by the good correlation obtained between $\log K_{ow}$ and $\log K_{D}$ (Fig. 1). This can be attributed to that the presence of ionic strength and DOC attached onto PE surfaces in seawater contributed to hydrophobic interactions and this mechanism overweighs that of represented by 'e' and 's'. Furthermore, none of the coefficients were statistically significant in seawater (p > 0.05), while only 'c' and 's' were significant in freshwater (p < 0.05). Therefore, LSER approach may not be fully addressing the sorption mechanism between PCBs and MPs, which can be due to compounds' (i) very similar properties making it difficult to be differentiated from each other; (ii) insignificant interactions with MPs. A similar comment could also be made for other families of compounds, regardless of their ionization status, such as perfluoroalkyl carboxylic acids (PFCAs) (Hatinoglu et al., 2023). Furthermore, it is unrealistic to extend the findings to every MPs-OCs combination due to the inconsistency of training datasets across studies. For example, Wei et al. (2019) trained their models that predict the adsorption by PE MPs with both ionic and neutral OCs by overlooking the difference in model domains for seawater and freshwater. In contrast, we kept the model domains the same for different water types to clearly study the water impact by changing only one variable at a time. As a result, the descriptors driving the models in our study differed from theirs, except 'v' being the dominant coefficient in both studies, which has the highest coverage of interactions.

4. Conclusion

Poly-parameter LSER equations were developed for the sorption of neutral aromatic OCs by MPs to investigate the effect of compounds' MW cutoff, MPs' polymer type, and water type on the sorption mechanism. This study extensively investigates the complex interactions occurring between MPs, OCs, and water components, and reveals the following major outcomes. First, as MW cutoff gets smaller, model's prediction strength increases. However, the relative importance of the intermolecular interactions stays the same throughout the cutoffs (except for < 544 g/mol), emphasizing the fact that the model is comprehensive enough to predict diverse compounds. Furthermore, neutral aromatic OCs with MWs smaller than 404 g/mol are not distinctive enough to change the direction of the sorptive interactions. Second, the internally and externally validated benchmark model (MW < 404 g/mol, n = 28) makes strong predictions for the sorption of neutral aromatic OCs by PE MPs in DI water with $R^2=0.85,\,RMSE=$ 0.38, $Q_{LOO}^2 = 0.73$ and $RMSE_{LOO} = 0.51$. Third, the comparison between the models for PE and PS shows that the benzene ring of the polymer does not govern the compounds' (n = 22) affinity towards them in DI water. Fourth, hydrophobicity is the predominant mechanism covered by LSER models that alters the sorption affinity of PCBs towards PE MPs in different water types.

Further research is warranted to extend the findings to environmentally realistic MPs to account for the impact of surface weathering and biofilm formation. Furthermore, increasing the diversity of compounds in datasets can significantly improve our understanding and prediction of environmentally relevant fate of compounds. Therefore, LSER descriptors should be generated for ionizable compounds by experimentally or computationally correcting those available for neutral forms of compounds. Moreover, sorption experiments in literature mostly lack in providing MP properties, which makes it challenging to investigate the mechanism. Future studies should systematically report all necessary properties to clarify the understanding of scientific

community.

Declaration of Competing Interest

The authors declare the following financial interests/personal relationships which may be considered as potential competing interests: Onur Apul reports financial support was provided by National Science Foundation.

Data availability

Data will be made available on request.

Acknowledgements

This work was supported by National Science Foundation through ECS 2003859 and 2004160 and Scientific and Technological Research Council of Turkey (TUBITAK) Project No: 220N044. The manuscript has not been subjected to the peer and policy review of the agency and therefore does not necessarily reflect their views. The authors are sincerely thankful for the contributions of Gokce Ciftci, Yaren Ozen, Dide Turkeli in collection of experimental data.

Appendix A. Supplementary data

Supplementary data to this article can be found online at https://doi.org/10.1016/j.ces.2023.119233.

References

- Apul, O.G., 2014. Predictive model development for adsorption of organic contaminants by carbon nanotubes. University of Clemson. PhD.
- Apul, O.G., Wang, Q., Shao, T., Rieck, J.R., Karanfil, T., 2013. Predictive Model Development for Adsorption of Aromatic Contaminants by Multi-Walled Carbon Nanotubes. Environ. Sci. Tech. 47, 2295–2303. https://doi.org/10.1021/es3001689.
- Apul, O.G., Zhou, Y., Karanfil, T., 2015. Mechanisms and modeling of halogenated aliphatic contaminant adsorption by carbon nanotubes. J. Hazard. Mater. 295, 138–144. https://doi.org/10.1016/j.jhazmat.2015.04.030.
- Apul, O.G., Perreault, F., Ersan, G., Karanfil, T., 2020. Linear solvation energy relationship development for adsorption of synthetic organic compounds by carbon nanomaterials: An overview of the last decade. Environ Sci (Camb). 6, 2949–2957. https://doi.org/10.1039/d0ew00644k.
- ASTM, Standard test methods for particle-size distribution (gradation) of soils using sieve analysis. ASTM D6913- 1900 PA: ASTM International, 2017.
- Atugoda, T., Wijesekara, H., Werellagama, D.R.I.B., Jinadasa, K.B.S.N., Bolan, N.S., Vithanage, M., 2020. Adsorptive interaction of antibiotic ciprofloxacin on polyethylene microplastics: Implications for vector transport in water. Environ. Technol. Innov. 19, 100971.
- Botterell, Z.L.R., Beaumont, N., Dorrington, T., Steinke, M., Thompson, R.C., Lindeque, P. K., 2019. Bioavailability and effects of microplastics on marine zooplankton: A review. Environ. Pollut. 245, 98–110. https://doi.org/10.1016/j.envpol.2018.10.065.
- Crawford, C.B., Quinn, B., 2016. Microplast. Pollutants. https://doi.org/10.1016/c2015-0-04315-5.
- Ding, H., Chen, C., Zhang, X., 2016. Linear solvation energy relationship for the adsorption of synthetic organic compounds on single-walled carbon nanotubes in water. SAR QSAR Environ. Res. 27, 31–45. https://doi.org/10.1080/ 1062936X.2015.1132764.
- Dong, J., Kang, Y., Kuang, S., Ma, H., Li, M., Xiao, J., Wang, Y., Guo, Z., Wu, H., 2023. Combined biological effects of polystyrene microplastics and phenanthrene on Tubifex tubifex and microorganisms in wetland sediment. Chem. Eng. J. 462, 142260 https://doi.org/10.1016/j.cej.2023.142260.
- Egert, T., Langowski, H.-C., 2022. Linear solvation energy relationships (LSERs) for robust prediction of partition coefficients between low density polyethylene and water. Part I: Experimental partition coefficients and model calibration. Eur. J. Pharm. Sci. 172. 106137.
- Egert, T., Langowski, H.-C., 2022. Linear solvation energy relationships (LSERs) for robust prediction of partition coefficients between low density polyethylene and water. Part II: Model evaluation and benchmarking. Eur. J. Pharm. Sci. 172, 106138.
- Endo, S., Koelmans, A.A., 2016. Sorption of hydrophobic organic compounds to plastics in the marine environment: equilibrium. In: Takada, H., Karapanagioti, H.K. (Eds.), Hazardous Chemicals Associated With Plastics in the Marine Environment. Springer.
- Ersan, G., Apul, O.G., Karanfil, T., 2016. Linear solvation energy relationships (LSER) for adsorption of organic compounds by carbon nanotubes. Water Res. 98, 28–38. https://doi.org/10.1016/j.watres.2016.03.067.

- Ersan, G., Apul, O.G., Karanfil, T., 2019. Predictive models for adsorption of organic compounds by Graphene nanosheets: comparison with carbon nanotubes. Sci. Total Environ. 654, 28–34. https://doi.org/10.1016/j.scitotenv.2018.11.029.
- Galloway, T.S., Cole, M., Lewis, C., 2017. Interactions of microplastic debris throughout the marine ecosystem. Nat. Ecol. Evol. 1, 1–8. https://doi.org/10.1038/s41559-017-0116
- Hartmann, N.B., Rist, S., Bodin, J., Jensen, L.H.S., Schmidt, S.N., Mayer, P., Meibom, A., Baun, A., 2017. Microplastics as vectors for environmental contaminants: Exploring sorption, desorption, and transfer to biota. Integr. Environ. Assess. Manag. 13, 488–493. https://doi.org/10.1002/ieam.1904.
- Hatinoglu, M.D., Perreault, F., Apul, O.G., 2023. Modified linear solvation energy relationships for adsorption of perfluorocarboxylic acids by polystyrene microplastics. Sci. Total Environ. 860, 160524.
- Huang, W., Deng, J., Liang, J., Xia, X., 2023. Comparison of lead adsorption on the aged conventional microplastics, biodegradable microplastics and environmentallyrelevant tire wear particles. Chem. Eng. J. 460, 141838 https://doi.org/10.1016/j. cei.2023.141838.
- Hüffer, T., Endo, S., Metzelder, F., Schroth, S., Schmidt, T.C., 2014. Prediction of sorption of aromatic and aliphatic organic compounds by carbon nanotubes using polyparameter linear free-energy relationships. Water Res. 59, 295–303. https://doi.org/ 10.1016/j.watres.2014.04.029.
- Hüffer, T., Weniger, A.K., Hofmann, T., 2018. Sorption of organic compounds by aged polystyrene microplastic particles. Environ. Pollut. 236, 218–225. https://doi.org/ 10.1016/j.envpol.2018.01.022.
- Lei, L., Wu, S., Lu, S., Liu, M., Song, Y., Fu, Z., Shi, H., Raley-Susman, K.M., He, D., 2018. Microplastic particles cause intestinal damage and other adverse effects in zebrafish Danio rerio and nematode Caenorhabditis elegans. Sci. Total Environ. 619–620, 1–8. https://doi.org/10.1016/j.scitotenv.2017.11.103.
- Li, J., Zhang, K., Zhang, H., 2018. Adsorption of antibiotics on microplastics. Environ. Pollut. 237, 460–467. https://doi.org/10.1016/j.envpol.2018.02.050.
- Liu, S., Deng, W.-K., Niu, S.-H., Mo, C.-H., Liao, X.-D., Xing, S.-C., 2023. Doxycycline combined manure microbes to enhances biofilm formation of the soil plastisphere and increases the surface bio-risk of microplastics vehicle. Chem. Eng. J. 454, 140530
- Llorca, M., Schirinzi, G., Martínez, M., Barceló, D., Farré, M., 2018. Adsorption of perfluoroalkyl substances on microplastics under environmental conditions. Environ. Pollut. 235, 680–691. https://doi.org/10.1016/j.envpol.2017.12.075.
- Ma, J., Zhao, J., Zhu, Z., Li, L., Yu, F., 2019. Effect of microplastic size on the adsorption behavior and mechanism of triclosan on polyvinyl chloride. Environ. Pollut. 254, 113104.
- Mei, W., Chen, G., Bao, J., Song, M., Li, Y., Luo, C., 2020. Interactions between microplastics and organic compounds in aquatic environments: A mini review. Sci. Total Environ. 736, 139472.
- Midi, H., Sarkar, S.K., Rana, S., 2010. Collinearity diagnostics of binary logistic regression model. J. Interdiscip. Math. 13, 253–267. https://doi.org/10.1080/ 09720502.2010.10700699.
- Pedà, C., Caccamo, L., Fossi, M.C., Gai, F., Andaloro, F., Genovese, L., Perdichizzi, A., Romeo, T., Maricchiolo, G., 2016. Intestinal alterations in European sea bass Dicentrarchus labrax (Linnaeus, 1758) exposed to microplastics: Preliminary results. Environ. Pollut. 212, 251–256. https://doi.org/10.1016/j.envpol.2016.01.083.
- Plastics Europe, Plastics the Facts 2021 An analysis of European plastics production, demand and waste data, 2021.
- Prajapati, A., Narayan Vaidya, A., Kumar, A.R., 2022. Microplastic properties and their interaction with hydrophobic organic contaminants: a review. Environ. Sci. Pollut. Res. 29, 49490–49512. https://doi.org/10.1007/s11356-022-20723-y.
- Rainieri, S., Conlledo, N., Larsen, B.K., Granby, K., Barranco, A., 2018. Combined effects of microplastics and chemical contaminants on the organ toxicity of zebrafish (Danio rerio). Environ. Res. 162, 135–143. https://doi.org/10.1016/j.envres.2017.12.019.
- Ricardo, I.A., Alberto, E.A., Silva Júnior, A.H., Macuvele, D.L.P., Padoin, N., Soares, C., Gracher Riella, H., Starling, M.C.V.M., Trovó, A.G., 2021. A critical review on microplastics, interaction with organic and inorganic pollutants, impacts and effectiveness of advanced oxidation processes applied for their removal from aqueous matrices. Chem. Eng. J. 424, 130282.
- Rochman, C.M., Brookson, C., Bikker, J., Djuric, N., Earn, A., Bucci, K., Athey, S., Huntington, A., McIlwraith, H., Munno, K., de Frond, H., Kolomijeca, A., Erdle, L., Grbic, J., Bayoumi, M., Borrelle, S.B., Wu, T., Santoro, S., Werbowski, L.M., Zhu, X., Giles, R.K., Hamilton, B.M., Thaysen, C., Kaura, A., Klasios, N., Ead, L., Kim, J., Sherlock, C., Ho, A., Hung, C., 2019. Rethinking microplastics as a diverse contaminant suite. Environ. Toxicol. Chem. 38, 703–711. https://doi.org/10.1002/etc.4371
- Schell, T., Rico, A., Cherta, L., Nozal, L., Dafouz, R., Giacchini, R., Vighi, M., 2022. Influence of microplastics on the bioconcentration of organic contaminants in fish: Is the "Trojan horse" effect a matter of concern? Environ. Pollut. 306, 119473 https://doi.org/10.1016/j.envpol.2022.119473.
- Scott, J.W., Gunderson, K.G., Green, L.A., Rediske, R.R., Steinman, A.D., 2021. Perfluoroalkylated substances (PFAS) associated with microplastics in a lake environment. Toxics. 9 (5), 106.
- Shan, S., Zhao, Y., Tang, H., Cui, F., 2017. Linear solvation energy relationship to predict the adsorption of aromatic contaminants on graphene oxide. Chemosphere 185, 826–832. https://doi.org/10.1016/j.chemosphere.2017.07.062.
- Shen, M., Song, B., Zeng, G., Zhang, Y., Teng, F., Zhou, C., 2021. Surfactant changes lead adsorption behaviors and mechanisms on microplastics. Chem. Eng. J. 405, 126989.
- Su, P.-H., Kuo, D.T.F., Shih, Y.-H., Chen, C.-y., 2018. Sorption of organic compounds to two diesel soot black carbons in water evaluated by liquid chromatography and polyparameter linear solvation energy relationship. Water Res. 144, 709–718.

- Sun, Y., Liu, S., Wang, P., Jian, X., Liao, X., Chen, W.-Q., 2022. China's roadmap to plastic waste management and associated economic costs. J. Environ. Manage. 309, 114686
- Uber, T.H., Hüffer, T., Planitz, S., Schmidt, T.C., 2019. Sorption of non-ionic organic compounds by polystyrene in water. Sci. Total Environ. 682, 348–355. https://doi. org/10.1016/j.scitotenv.2019.05.040.
- Uber, T.H., Hüffer, T., Planitz, S., Schmidt, T.C., 2019. Characterization of sorption properties of high-density polyethylene using the poly-parameter linearfree-energy relationships. Environ. Pollut. 248, 312–319. https://doi.org/10.1016/j. envpol.2019.02.024.
- N. Ulrich, S. Endo, T.N. Brown, N. Watanabe, G. Bronner, M.H. Abraham, K.-U. Goss, UFZ-LSER database v 3.2.1, (2022). http://www.ufz.de/lserd (accessed March 16, 2022)
- Vasanthi, R.L., Arulvasu, C., Kumar, P., Srinivasan, P., 2021. Ingestion of microplastics and its potential for causing structural alterations and oxidative stress in Indian green mussel Perna viridis—A multiple biomarker approach. Chemosphere 283, 130070
- Velzeboer, I., Kwadijk, C.J.A.F., Koelmans, A.A., 2014. Strong sorption of PCBs to nanoplastics, microplastics, carbon nanotubes, and fullerenes. Environ. Sci. Tech. 48, 4869–4876. https://doi.org/10.1021/es405721v.
- Wang, F., Shih, K.M., Li, X.Y., 2015. The partition behavior of perfluorooctanesulfonate (PFOS) and perfluorooctanesulfonamide (FOSA) on microplastics. Chemosphere 119, 841–847. https://doi.org/10.1016/j.chemosphere.2014.08.047.
- Wang, Y., Wang, X., Li, Y., Li, J., Liu, Y., Xia, S., Zhao, J., 2021. Effects of exposure of polyethylene microplastics to air, water and soil on their adsorption behaviors for copper and tetracycline. Chem. Eng. J. 404, 126412.

- Wei, X., Li, M., Wang, Y., Jin, L., Ma, G., Yu, H., 2019. Developing predictive models for carrying ability of micro-plastics towards organic pollutants. Molecules 24 (9), 1784.
 Wright, S.L., Rowe, D., Thompson, R.C., Galloway, T.S., 2013. Microplastic ingestion decreases energy reserves in marine worms. Curr. Biol. 23 (23), R1031–R1033.
- Wu, W., Yang, K., Chen, W., Wang, W., Zhang, J., Lin, D., Xing, B., 2016. Correlation and prediction of adsorption capacity and affinity of aromatic compounds on carbon nanotubes. Water Res. 88, 492–501. https://doi.org/10.1016/j.watres.2015.10.037.
- Xia, X.-R., Monteiro-Riviere, N.A., Riviere, J.E., 2010. An index for characterization of nanomaterials in biological systems. Nat. Nanotechnol. 5, 671–675. https://doi.org/ 10.1038/nnano.2010.164.
- Xu, J., Wang, L., Sun, H., 2021. Adsorption of neutral organic compounds on polar and nonpolar microplastics: Prediction and insight into mechanisms based on pp-LFERs. J. Hazard. Mater. 408, 124857.
- You, H., Huang, B., Cao, C., Liu, X., Sun, X., Xiao, L., Qiu, J., Luo, Y., Qian, Q., Chen, Q., 2021. Adsorption–desorption behavior of methylene blue onto aged polyethylene microplastics in aqueous environments. Mar. Pollut. Bull. 167, 112287.
- Zhang, H., Wang, J., Zhou, B., Zhou, Y., Dai, Z., Zhou, Q., Chriestie, P., Luo, Y., 2018. Enhanced adsorption of oxytetracycline to weathered microplastic polystyrene: Kinetics, isotherms and influencing factors. Environ. Pollut. 243, 1550–1557. https://doi.org/10.1016/j.envpol.2018.09.122.
- Zhang, X., Xia, M., Zhao, J., Cao, Z., Zou, W., Zhou, Q., 2022. Photoaging enhanced the adverse effects of polyamide microplastics on the growth, intestinal health, and lipid absorption in developing zebrafish. Environ. Int. 158, 106922.
- Zhou, Y., Apul, O.G., Karanfil, T., 2015. Adsorption of halogenated aliphatic contaminants by graphene nanomaterials. Water Res. 79, 57–67. https://doi.org/ 10.1016/j.watres.2015.04.017.